© 2017. Published by The Company of Biologists Ltd | Journal of Experimental Biology (2017) 220, 3621-3631 doi:10.1242/jeb.161638

RESEARCH ARTICLE

Skeletal stiffening in an amphibious fish out of water is a response to increased body weight

Andy J. Turko[1,*], Dietmar Kültz[2], Douglas Fudge[1,3], Roger P. Croll[4], Frank M. Smith[5], Matthew R. Stoyek[4,5] and Patricia A. Wright[1]

ABSTRACT

Terrestrial animals must support their bodies against gravity, while aquatic animals are effectively weightless because of buoyant support from water. Given this evolutionary history of minimal gravitational loading of fishes in water, it has been hypothesized that weight-responsive musculoskeletal systems evolved during the tetrapod invasion of land and are thus absent in fishes. Amphibious fishes, however, experience increased effective weight when out of water – are these fishes responsive to gravitational loading? Contrary to the tetrapod-origin hypothesis, we found that terrestrial acclimation reversibly increased gill arch stiffness (~60% increase) in the amphibious fish *Kryptolebias marmoratus* when loaded normally by gravity, but not under simulated microgravity. Quantitative proteomics analysis revealed that this change in mechanical properties occurred via increased abundance of proteins responsible for bone mineralization in other fishes as well as in tetrapods. Type X collagen, associated with endochondral bone growth, increased in abundance almost ninefold after terrestrial acclimation. Collagen isoforms known to promote extracellular matrix cross-linking and cause tissue stiffening, such as types IX and XII collagen, also increased in abundance. Finally, more densely packed collagen fibrils in both gill arches and filaments were observed microscopically in terrestrially acclimated fish. Our results demonstrate that the mechanical properties of the fish musculoskeletal system can be fine-tuned in response to changes in effective body weight using biochemical pathways similar to those in mammals, suggesting that weight sensing is an ancestral vertebrate trait rather than a tetrapod innovation.

KEY WORDS: Body support, Biomechanics, Microgravity, Collagen remodelling, Phenotypic plasticity

INTRODUCTION

The invasion of land by aquatic vertebrates poses a fundamental physical problem: animals that were once buoyant in water become effectively heavier in air (Denny, 1993). Increased effective gravity in terrestrial environments is thought to have driven the evolution of robust and responsive musculoskeletal systems in tetrapods to provide postural support and improve locomotion (Clack, 2002). Tetrapod skeletons are also highly responsive to changes in mechanical load (Currey, 2002). In mammals, increased body weight or exercise causes gains in muscle mass and bone density while decreases in mechanical forces during bedrest or spaceflight have the opposite effect (Robling et al., 2006). Would fishes, with an evolutionary history of effective weightlessness in water, respond similarly to increased body weight (Horn, 2005; Martin, 2007)?

While most fishes never experience gravitational loading out of water, over 200 species of extant amphibious fishes experience increased effective weight during terrestrial sojourns (Ord and Cooke, 2016; Wright and Turko, 2016). If weight-induced skeletal plasticity evolved at the base of the tetrapod lineage, amphibious fishes should be unresponsive to gravitational loading and may thus be expected to possess constitutively stronger and stiffer support systems to provide reinforcement while out of water. Alternatively, if weight responsiveness is a fundamental characteristic of vertebrate bone or has convergently evolved in amphibious fishes, terrestrial acclimation should cause amphibious fishes to increase the strength and stiffness of skeletal support structures.

There is evidence that fish bones are responsive to extreme and dynamic mechanical loads, such as surgically implanted opercular springs (Atkins et al., 2015), vertebral lordosis (Kranenbarg et al., 2005), hard versus soft diets (Meyer, 1987; Huysseune et al., 1994) or cantilevered billfish rostra (Atkins et al., 2014). The effect of gravitational loading in fishes has not been studied, however. While mechanical loads caused by gravity are similar to those imparted by other, more routine sources (e.g. muscle contraction or crushing prey), they differ and may have been overlooked both because gravitational forces are relatively weak and because the nature of loading is static. For example, a common view has held that bone growth or resorption occurs only when mechanical loading of bone exceeds threshold levels, and the force of gravity would not be sufficient to surpass these thresholds (McBride and Silva, 2012). However, recent evidence suggests that these thresholds do not exist (Sugiyama et al., 2012; Christen et al., 2014). Furthermore, dynamic or cyclical mechanical forces are thought to be the predominant signals for bone growth and mineralization, and gravitational loading of inactive fish out of water (e.g. Turko et al., 2014) would be largely static and therefore may not be expected to cause a typical skeletal loading response (Turner, 1998; Yang et al., 2006).

The objective of this study was to determine whether there is a cellular response in the skeleton of amphibious fishes experiencing mechanical loading owing to increased effective gravity when out of water. These experiments allowed us to test a critical prediction made by the 'weight-insensitive fish hypothesis' – that amphibious fishes should not respond to increased effective body weight because weight-sensitive musculoskeletal systems evolved during the tetrapod invasion of land. In contrast, evidence that amphibious fishes respond to gravitational loading using similar biochemical

[1]Department of Integrative Biology, University of Guelph, 50 Stone Road East, Guelph, ON, Canada N1G 2W1. [2]Department of Animal Sciences, University of California, Davis, 1 Shields Ave., Meyer Hall, Davis, CA 95616, USA. [3]Schmid College of Science and Technology, Chapman University, 1 University Dr., Orange, CA 92866, USA. [4]Department of Physiology and Biophysics, Dalhousie University, 5850 College Street, Halifax, Nova Scotia, Canada B3H 4R2. [5]Department of Medical Neuroscience, Dalhousie University, 5850 College Street, Halifax, Nova Scotia, Canada B3H 4R2.

*Author for correspondence (aturko@uoguelph.ca)

A.J.T., 0000-0002-6330-5798

Received 24 April 2017; Accepted 7 August 2017

Journal of Experimental Biology (2017) 220, 3621-3631 doi:10.1242/jeb.161638

pathways as tetrapods would be strong evidence that weight-responsiveness is an ancestral character of vertebrate skeletal tissue. Mangrove rivulus (*Kryptolebias marmoratus*) provided an ideal experimental model for our studies: these fish can survive terrestrially for several months (Taylor, 2012), have a sequenced genome (Kelley et al., 2016) and predicted proteome, and are small enough to fit into a random positioning machine to experience simulated microgravity on Earth. By terrestrially acclimating fish while effectively weightless, we could tease apart the effect of gravity from other confounding effects of terrestrial acclimation. We focused on weight-induced plasticity of the gill arches using mechanical testing, quantitative proteomics and histology. Gill arches were chosen because of their relatively simple skeletal support, provided by the long and slender ceratobranchial bone, and lack of involvement in locomotion or other behaviours that differ between aquatic and terrestrial environments. Skeletal plasticity of the pectoral girdle in response to walking versus swimming has been observed in *Polypterus senegalus*, for example (Standen et al., 2014), but our aim was to separate the impact of altered effective weight from plasticity resulting from different patterns of musculoskeletal use (DiGirolamo et al., 2013).

MATERIALS AND METHODS

Animals

Captive-reared mangrove rivulus, *Kryptolebias marmoratus* (Poey 1880), originating from Belize (lineage 50.91; Tatarenkov et al., 2010) were obtained from a breeding colony maintained at the University of Guelph (19.3±0.1 mm, 82.1±1.5 mg). Fish were housed under standard conditions described elsewhere (Frick and Wright, 2002). Zebrafish, *Danio rerio* (Hamilton 1822), were obtained from the pet trade to provide comparison with fully aquatic fish of similar body size (20.8±0.8 mm, 93.4±9.6 mg). All experiments were approved by the University of Guelph animal care committee (animal utilization protocols 2239 and 2478).

Terrestrial acclimation

Adult mangrove rivulus were terrestrially acclimated (25°C) on damp filter paper soaked with 15‰ water as described previously (Ong et al., 2007). For proteomics and transmission electron microscopy (TEM) experiments, fish were terrestrially acclimated for 14 days and compared with control fish held in 15‰ brackish water. To determine the effect of terrestrial acclimation on the mechanical properties and collagen composition of gill arches, fish were divided into five treatment groups: control (15‰ water), 7 or 14 days of terrestrial exposure, or 14 days terrestrial exposure followed by recovery (14 days or 12 weeks) in water. Body length and mass were similar between treatment groups (P>0.05).

Mechanical testing

The force required to deform individual gill arches was measured using a custom tensile testing apparatus (Fudge et al., 2003). Briefly, gill arches dissected from the left side were separated by cutting through each epibranchial and hypobranchial bone (dorsal and ventral extremities). Separated gill arches were held in 15‰ brackish water with 0.1 mmol l^{-1} phenylmethylsulfonyl fluoride to minimize protein degradation prior to tensile testing; all tests were completed within ∼45 min of euthanasia. Individual gill arches were mounted using cyanoacrylate gel between a glass microbeam (force transducer) and a fine tungsten point epoxied to a micrometer (Fig. 1A). Retraction of the micrometer caused the glass rod to bend and the gill arch to stretch and deform. Tensile tests were filmed through a dissecting microscope (MD200 microscope camera, AmScope, Irvine, CA; 2 frames s^{-1}) and quantified using ImageJ (Schneider et al., 2012).

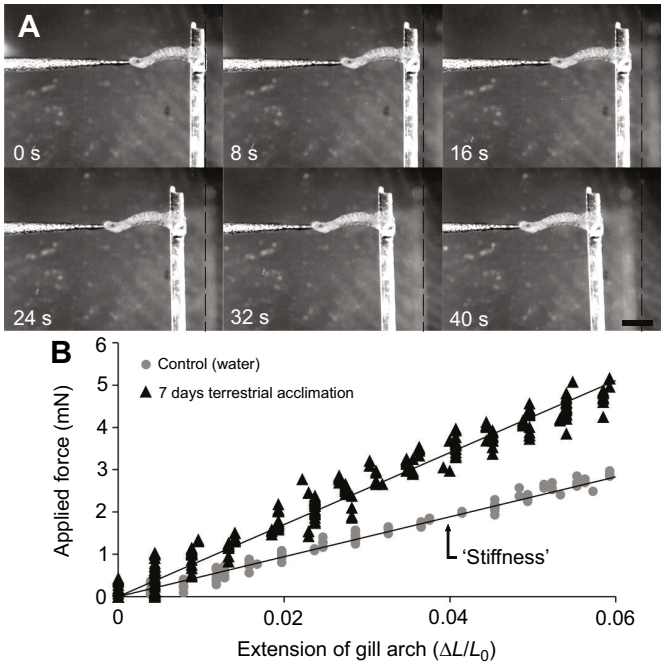

Fig. 1. Mechanical testing of mangrove rivulus gill arches. (A) Representative video frames, 8 s apart, showing the glass microbeam force transducer used to measure stiffness of isolated gill arches; the vertical dashed line indicates the starting position of the microbeam for comparison between frames. Scale bar, 1 mm. (B) Representative force–extension curves for one individual gill arch from a water-acclimated fish (grey circles) and a terrestrially acclimated fish (black triangles) used to calculate mechanical properties. Gill extension was calculated as the change in length (ΔL) divided by the initial length (L_0).

Applied forces were calculated from the deflection of the glass microbeam using beam theory (Fudge et al., 2003). Extension of the gill arch (a combination of stretching and deformation) was calculated by taking the linear distance between each end of the arch in each video frame. Because of variation in cross-sectional size and shape along the length of the gill arches, we were unable to meaningfully calculate traditional stiffness (standardized to cross-sectional area). Instead, effective 'stiffness' of the whole gill arch was calculated as the slope of the force–extension curve from 0 to 5% extension and is presented in newtons (N), or calculated as a spring constant from the slope of the force–length curves (N mm^{-1}). All four gill arches were tested in the time-course experiment; only the first two gill arches were tested after microgravity acclimation as these were larger, easier to handle and all four gill arches responded to terrestrial acclimation in the same way (i.e. there was no significant treatment by arch interaction, P>0.05).

Microgravity simulation

Mangrove rivulus were acclimated to simulated microgravity (25°C, 12 h:12 h light:dark) for 7 days using a desktop random positioning machine (RPM; Airbus Defence and Space, Leiden, Netherlands) that simulates microgravity by rotating animals randomly about two axes so that the mean vector force of gravity over time approaches zero (Borst and van Loon, 2009; Herranz et al., 2013; Wuest et al., 2015). We assumed that the gill arches deformed more slowly than the gravitational vector changed, which would reduce the amount of strain that the arches experienced in the RPM compared with the terrestrially acclimated fish maintained at 1 ***g***. In contrast, if the gill arches

deformed faster than the rate of rotation by the random positioning machine, we would expect to see stiffening as the arches would continuously experience strain from gravity acting in an ever-shifting, random vector, assuming these deformations occurred slowly enough to be sensed (Ueki et al., 2008). The RPM was operated in 'real random' mode, with both direction and intervals of rotation randomized, and the maximum angular velocity=20 deg s^{-1}, minimum angular velocity=8 deg s^{-1} and acceleration=30 deg s^{-2}. An onboard accelerometer and proprietary software calculated that we maintained a simulated effective gravity of 0.06 ***g*** throughout the experiment, slightly less than half of the gravity experienced on the moon (0.16 ***g***; Hirt and Featherstone, 2012).

Microgravity-acclimated animals were housed under terrestrial conditions in standard six-well plates with a corrugated bottom lined with gauze soaked in brackish water. This allowed fish to move freely within a well without 'tumbling' during rotation, confirmed by video recording (Movie 1). Activity was quantified from 1 h recording periods at 1 h, 24 h, 3 days and 7 days as the proportion of video frames in which a body movement occurred. Control (1 g) fish, in water or air, were placed in identical six-well plates located beside the RPM to ensure these fish experienced a similar environment as the microgravity-acclimated fish. After 7 days, fish were euthanized with an overdose of MS222 and the mechanical properties of gill arches were measured.

Proteomics

Mangrove rivulus (control, n=6; 14 days terrestrial exposure, n=6) were euthanized with an overdose of MS222 and gill baskets were dissected, snap-frozen in liquid nitrogen and stored at −80°C until analysis. Protein extraction, protein assays and in-solution trypsin digestion were performed as reported previously (Kültz et al., 2013). Tryptic peptides from each sample (200 ng total) were injected with a nanoAcquity sample manager (Waters, Milford, MA, USA) and trapped for 1 min at 15 µl min^{-1} on a Symmetry trap column (Waters 186003514). They were then separated on a 1.7 µm particle size BEH C18 column (250 mm×75 µm, Waters 186003545) using a 125-min linear gradient ranging from 3% to 35% acetonitrile by reversed phase liquid chromatography using a nanoAcquity UPLC (Waters). Nano-electrospray ionization (nESI) was achieved by elution from a pico-emitter tip (New Objective FS360–20-10-D-20, Woburn, MA, USA) into an nESI source fitted on an ImpactHD UHR-QTOF mass spectrometer (Bruker Daltonics, Bremen, Germany). Batch-processing of samples was controlled with Hystar 3.2, and peak lists were generated with DataAnalysis 4.2 (Bruker Daltonics) using data-dependent acquisition as previously described (Kültz et al., 2015).

To identify gill proteins, raw data were imported into PEAKS Studio 8.0 (BSI, Waterloo, Canada) followed by charge state deconvolution, deisotoping and peak list generation. PEAKS 8.0, Mascot 2.2.7 (Matrix Science, London, UK; version 2.2.07) and X! Tandem Cyclone (www.thegpm.org/tandem/) search engines were used to identify proteins from MSMS spectra using trypsin as the enzyme, and maximum of one missed cleavage permitted, Cys carbamidomethylation, Met oxidation, Pro hydroxylation, *N*-terminal carbamylation and *N*-terminal acetylation as variable modifications. The precursor ion mass tolerance was set to 20 ppm (100 ppm for X! Tandem searches) and fragment ion mass tolerance was set to 0.02 amu. The *K. marmoratus* proteome (38,516 sequences) was downloaded on 5 July 2016 from NCBI and decoy entries were added for each sequence by PEAKS 8.0. The resulting database containing 77,032 total entries was used for all searches to determine protein false discovery rate (FDR). Results from all three search engines were consolidated in Scaffold 4.4 (Proteome Software Inc., Portland, OR, USA) with peptide identifications being accepted if FDR <0.1%. Protein identifications were accepted FDR <1.0% and contained at least one identified peptide. Proteins that contained similar peptides and could not be differentiated based on MS/MS analysis alone were grouped into clusters by the Scaffold software to satisfy the principles of parsimony. Label-free quantitative profiling of peptide intensities and calculation of relative protein abundances in each sample was performed with PEAKS 8.0 using the following parameters: FDR <1%, confident samples per peptide ≥4, mass error tolerance=30 ppm and retention time shift tolerance=3 min.

Histology

The collagen-specific dye Picrosirius Red (Electron Microscopy Sciences, Hatfield, PA, USA) was used to determine the density and/or thickness of collagen fibres in sections of gill arches and filaments. Gill arches were fixed overnight (4°C) in 10% buffered formalin, decalcified (Cal-Ex, Fisher Scientific) for 1 h (room temperature) and double-embedded in 2% agar followed by paraffin wax to aid tissue orientation. Cross-sections (3 µm for gill arch analysis, 5 µm for filaments) were cut through the middle of the ceratobranchial bone of each gill arch, the main skeletal support structure. Tissues were stained with Picrosirius Red and photographed under circularly polarized light as previously described (Johnson et al., 2014). Under polarized light, thin and/or disorganized collagen appears green, while densely packed collagen appears red (Rich and Whittaker, 2005). Instead of separating collagen hues into arbitrary colour 'bins' as described previously (MacKenna et al., 1994; Rich and Whittaker, 2005; Johnson et al., 2014), we simply calculated the mean hue of collagen-staining pixels in each gill arch after normalizing the 256 colour histogram so that the lowest-intensity green was scored with a value of 1 (traditionally, hue value=127) while the most intense red pixels received a score of 155 (traditionally, hue value=229).

TEM was used to describe the structure of gill arch and filament extracellular matrix. Gills were rapidly dissected from euthanized fish (control n=2, 14 days air exposure n=2) and immediately fixed in freshly prepared 2% glutaraldehyde/2% tannic acid in 0.1 mol l^{-1} cacodylate buffer (pH 7.4) as previously described (King et al., 1989). Gill arches were washed (3×, 0.5 mol l^{-1} HEPES), post-fixed in 1% osmium tetroxide (2 h), washed (3×, 0.5 mol l^{-1} HEPES), stained in 2% uranyl acetate (2 h) and then dehydrated through a graded ethanol series. Samples were then infiltrated with a descending series of ethanol:LR White resin (Electron Microscopy Sciences), put into capsules and cured (24 h, 60°C). Thin sections (100 nm) were mounted on mesh copper grids coated with a layer of Formvar/carbon (Electron Microscopy Sciences) and post-stained with 2% uranyl acetate followed by lead citrate. Images were obtained using a Philips CM10 electron microscope (80 kV) equipped with an Olympus/SIS Morada top mount 11MP CCD camera.

Calcium content of gill baskets

Gill baskets from five individuals were rapidly dissected from euthanized fish and pooled for a single sample. Samples were dried (65°C, 24 h), weighed and then digested with 3:1 trace metal grade HNO_3:HCl for 3 h. Digested samples were heated (90°C, 2 h) and filtered, and calcium content was measured using flame atomic absorption spectrometry (Varian SpectrAA 220 double beam flame atomic absorption spectrometer, Agilent Technologies, Santa Clara, CA, USA). Bone mineral density was approximated assuming all calcium was present in the form of hydroxyapatite

Journal of Experimental Biology (2017) 220, 3621-3631 doi:10.1242/jeb.161638

$[Ca_5(PO_4)_3(OH)]$, the main mineral component of bone. Hydroxyapatite is 39.9% calcium by mass, thus bone mineral density was calculated by dividing the measured calcium content by this fraction (0.399).

Statistical analyses

Two-way repeated-measures ANOVAs were used to detect differences in mechanical properties and collagen density between gill arches and across treatment groups. In a few instances, dissected gill arches were lost or contaminated with cyanoacrylate and excluded from all analyses. Data were natural-logarithm (ln) transformed when necessary to meet assumptions of normality and equal variance. Statistical significance for label-free quantitation is based on PEAKSQ $-\log_{10}P$-values, which have been calculated using a previously developed algorithm that has been optimized for proteomics data (Cox and Mann, 2008). A significance threshold of $-\log_{10}P$-value ≥5 and fold change of ≥1.5 were applied. To clarify visualization of protein abundances, values were *z*-score transformed (mean protein abundance was subtracted from each individual value, and the result was divided by the standard deviation) to normally distribute abundances and enhance the dynamic range for each protein (Berrar et al., 2007).

RESULTS

Mechanical properties of gill arches

Applying force to isolated gill arches caused both small changes in shape (i.e. straightening) and straining of the gill skeleton. Together, these deformations provided an overall measure of the lengthening of the gill arch. The amount of force required to extend the gill arches significantly increased after 7 days of acclimation out of water when calculated from both force–extension curves ($P<0.001$; Figs 1B and 2A) and force–length curves ($P<0.001$; Fig. S1). No additional increase in gill arch stiffness was observed after a further 7 days of terrestrial acclimation. Increased gill arch stiffness persisted after a 14 day recovery period in water, but returned to control values after 12 weeks (Fig. 2A, Fig. S1). The fourth gill arch was significantly stiffer than arches 1 or 2 (force–extension $P=0.002$; Fig. 2B; force–length $P<0.001$; Fig. S1), possibly because arch 4 was straighter at the outset. The stiffening we observed in terrestrially acclimated fish was widespread across all four gill arches (interaction $P>0.05$; Fig. 2A, Fig. S1).

Terrestrially acclimated fish held under conditions of simulated microgravity showed no obvious ill effects, and activity was similar to that of terrestrially acclimated fish at 1 ***g*** ($P>0.05$; Fig. S2). Microgravity-acclimated fish showed no righting response when inverted, which could have negated the effect of the random rotations by allowing gravity to act on the gill arches in a consistent vector (Movie 1). Gill arches from terrestrially acclimated fish in simulated microgravity were of comparable stiffness to those from control fish in water ($P>0.05$; Fig. 2B, Fig. S3). Terrestrially acclimated fish placed at the base of the random positioning machine to control for effects of noise and vibration had significantly stiffer gill arches relative to fish in water, as observed in the time course experiment (force–extension $P=0.001$; Fig. 2B; force–length $P=0.025$; Fig. S3).

To determine whether gill arches from the amphibious *K. marmoratus* are constitutively stiffer than gills in fully aquatic fishes, we tested the mechanical properties of gill arches from similarly sized *D. rerio*. Overall, gill arches of control *K. marmoratus* in water were significantly stiffer than those of *D. rerio* (force–extension $P=0.002$; Fig. 3; force–length $P=0.006$; Fig. S4). There was no significant effect of gill arch when 'stiffness' was calculated from force–extension curves ($P>0.05$, interaction $P>0.05$), but the fourth gill arch of both species was significantly stiffer than the first using force–length calculations ($P=0.012$, interaction $P>0.05$).

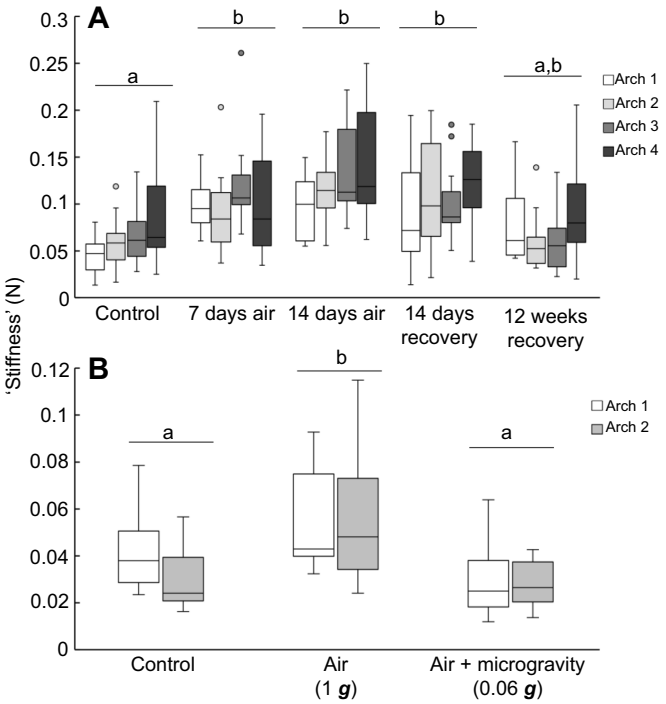

Fig. 2. Increased gill stiffness after terrestrial acclimation is reversible in *Kryptolebias marmoratus*. (A) Force required to deform all four gill arches from the left side of control fish in water ($n=15$), after 7 days ($n=13$) or 14 days in air ($n=13$), or 14 days in air followed by 14 days ($n=12$) or 12 weeks ($n=12$) recovery in water. (B) Force required to deform gill arches 1 and 2 in fish acclimated to water at 1 ***g*** ($n=12$), 7 days in air at 1 ***g*** ($n=12$) or 7 days in simulated microgravity (0.06 ***g***; $n=10$). Different letters above treatment groups denote significant effects of treatment (two-way repeated-measures ANOVA and Holm–Sidak *post hoc* tests, $P\leq0.001$).

Proteomic responses to terrestrial acclimation

Quantitative proteomics analysis of gill tissue identified 1095 proteins, 152 of which significantly changed in abundance after 14 days of terrestrial acclimation. Of these differentially expressed

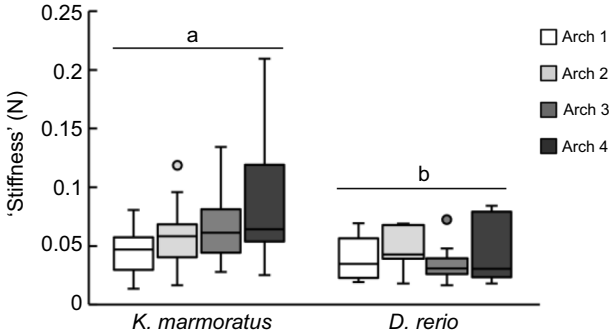

Fig. 3. Increased stiffness of *K. marmoratus* versus *Danio rerio* gill arches. Force required to deform gill arches from the left side of amphibious *K. marmoratus* acclimated to water ($n=15$) compared with those of the fully aquatic zebrafish ($n=9$). The *K. marmoratus* data presented here are the control values repeated from Fig. 2A for comparison. Different letters above treatment groups denote significant differences between species (two-way repeated-measures ANOVA and Holm–Sidak *post hoc* tests, $P=0.002$).

Journal of Experimental Biology

Journal of Experimental Biology (2017) 220, 3621-3631 doi:10.1242/jeb.161638

proteins, 23 were structural components of the cytoskeleton or extracellular matrix (Fig. 4). Many of the cytoskeletal proteins that increased in abundance are components of the microfilament network. These included actin, responsible for forming microfilaments, as well as several proteins that regulate the folding (T-complex) and bundling (plastin-3) of the actin cytoskeleton. Type II keratin, part of the intermediate filament network, also significantly increased in abundance after terrestrial acclimation (Fig. 4).

Collagen was particularly responsive to terrestrial acclimation; of the 34 collagen isoforms identified in the proteomics analysis, 71% increased in abundance (Table S1), significantly more than expected by chance (*Z*-test for proportions, P=0.016). Abundances of both alpha subunits of type I collagen, the major organic structural component of bone, increased significantly (P<0.001), but only by ~30% (relative to total protein abundance), below our *a priori* threshold for consideration. Considering the large absolute abundance of type I collagen in the gills (5.8±0.3% of total protein in control samples, 7.4±1.0% after 14 days terrestrial acclimation), this 30% increase nonetheless represents a considerable increase in the absolute number of collagen molecules present. Abundance of type X collagen, associated with bone formation, increased 8.8-fold (P<0.0001) after terrestrial acclimation (Fig. 4). Gills of terrestrially acclimated fish also showed increased abundance of collagen types IX and XII, isoforms that enhance cross-linking between extracellular matrix components (Fig. 4).

Morphological changes after terrestrial acclimation

We used polarized light imaging of Picrosirius-Red-stained cross-sections through the middle of the ceratobranchial bone to assess the relative density of collagen in the extracellular matrix. Collagen had a relatively green hue in control fish, indicating less densely packed molecules, while in terrestrially acclimated fish the gill arches had a significantly redder hue, indicative of more densely packed collagen (P=0.004; Fig. 5A,B). After recovery in water, the hue of gill arch collagen was intermediate and not statistically different from either control or terrestrially acclimated fish (P>0.05). Across all treatments, the third and fourth gill arches were significantly redder in hue than the first and second arches (P=0.012, interaction P>0.05). Consistent with both the proteomic data and polarized light imaging of cross-sections, TEM revealed densely packed collagen molecules at the margins of the ceratobranchial bones in terrestrially acclimated fish (Fig. 5C,D). Furthermore, a dark band of mineral was present in the ceratobranchial bone margin after terrestrial acclimation (Fig. 5D).

The gill filaments protrude perpendicularly from the gill arch and are supported by a cartilage rod produced by a central core of chondrocytes. Similar to the ceratobranchial bones, Picrosirius-Red-stained sections through the gill filaments were significantly redder in hue under polarized light after terrestrial acclimation (P<0.001; Fig. 6A). Electron micrographs of longitudinal sections through the filament-supporting cartilage rods showed denser aggregations of highly organized collagen in terrestrially acclimated fish (Fig. 6B,C), a pattern similar to what we observed in the gill arches.

Calcium content of whole gill baskets was very low (66.7±1.5 mg g^{-1} dry mass; Fig. 7A), but these measurements were consistent with the low degree of mineralization observed in electron micrographs of the gill skeleton (Fig. 7B). If we assume that this calcium is present as hydroxyapatite, the major mineral component of bone, this is equal to a mineral content of 16.7±0.4%. Gill basket calcium content did not change after terrestrial acclimation (P>0.05; Fig. 7A).

DISCUSSION

Our results are contrary to the hypothesis that vertebrate weight sensitivity evolved with the tetrapod invasion of land. Like astronauts moving between Earth and outer space (Robling et al., 2006), we found that the gill skeleton of the amphibious fish *K. marmoratus* is stiffened in response to increased effective weight, probably via both the modification of existing tissues and the formation of new endochondral bone. Furthermore, many of the protein-level changes we observed in the gills of terrestrially acclimated *K. marmoratus* were similar to those associated with increased body weight in tetrapods, such as increased abundances of collagen isoforms associated with endochondral bone formation and cross-linking of the extracellular matrix. These results suggest a fundamentally conserved response to changes in body weight in vertebrates.

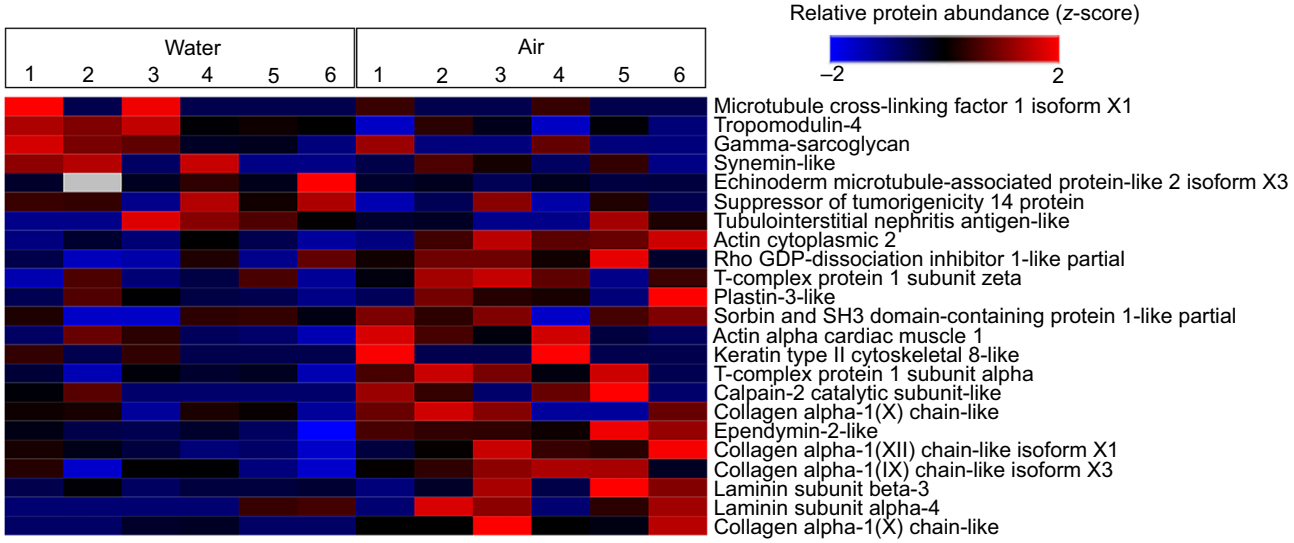

Fig. 4. Relative abundances of structural proteins that significantly changed expression after 2 weeks of terrestrial acclimation. Each column represents a single individual and each row a unique protein (control n=6, 14 days in air n=6). Red rectangles represent proteins that increased expression after terrestrial acclimation and blue represents proteins that were less abundant. Relative protein abundances were *z*-score transformed to normally distribute values within each row and make it easier to visualize differences between treatments.

Journal of Experimental Biology (2017) 220, 3621-3631 doi:10.1242/jeb.161638

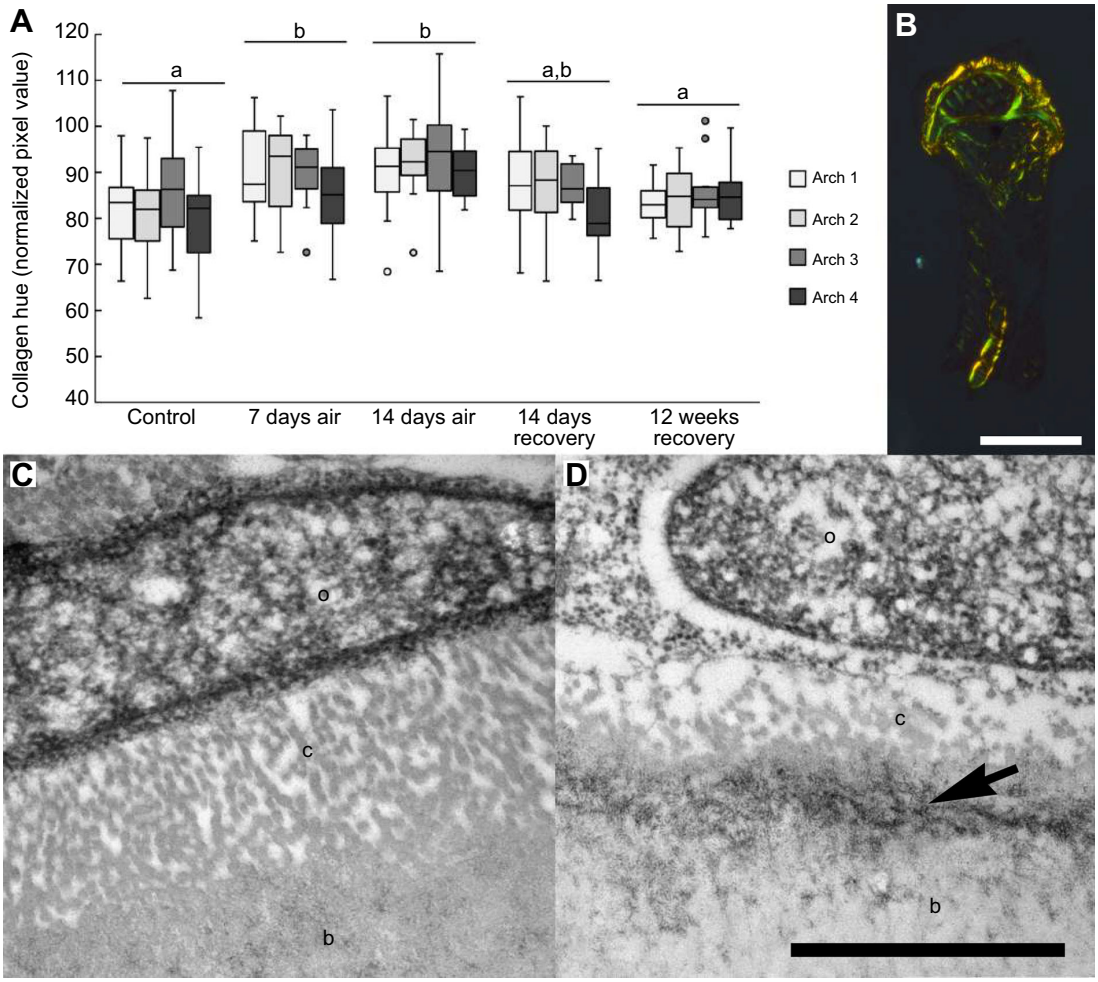

Fig. 5. Increased density of collagen molecules in *K. marmoratus* gill arches after terrestrial acclimation. (A) Boxplot showing the mean hue value of collagen observed in ceratobranchial bone cross-sections of control fish in water (n=15), after 7 days (n=13) or 14 days in air (n=13), or 14 days in air followed by 14 days (n=12) or 12 weeks (n=12) recovery in water. Larger values indicate larger and more densely packed collagen fibrils. Different letters above treatment groups denote significant effects of treatment (two-way repeated-measures ANOVA and Holm–Sidak *post hoc* tests, P=0.004). (B) Representative image of a control Picrosirius-Red-stained gill arch under polarized light used to measure collagen hue. Scale bar, 100 µm. (C,D) Representative transmission electron micrograph of a ceratobranchial bone from a control fish in water (C) and from a fish acclimated terrestrially for 14 days (D). Note the dark band of mineralized bone (arrow) and the especially dense packing of collagen (c) beneath the osteoblast (o) along the outer margin of the bone (b) in the terrestrially acclimated fish. Scale bar, 1 µm.

Weight responsiveness in an amphibious fish

Gill arches of terrestrially acclimated fish stiffened rapidly, within 1 week, and no further change in mechanical properties was observed after an additional week out of water. In most bone, desensitization to mechanical forces occurs within hours to days (Turner, 1998; Robling et al., 2001). Thus, it seems probable that extracellular matrix-synthesizing cells of the gill skeleton were desensitized to mechanical loading after 1 week of terrestrial acclimation. Alternatively, the stiffening that occurred within the first week may have been sufficient to support the increased weight of the gill arches, thus removing the stimulus for further plasticity (Robling et al., 2006). The increased gill stiffness caused by terrestrial acclimation persisted after 2 weeks of recovery in water, but was reversible after 3 months. The extended time required to reverse the terrestrially induced response is consistent with the normal rate of protein turnover in fishes (~1% per day in trout at 15°C; Lyndon and Houlihan, 1998) and suggests either that stiffened gill baskets do not impose a large and/or immediate cost or that *K. marmoratus* are not able to quickly decrease gill arch stiffness.

Stiffening of gill arches in terrestrially acclimated fish could have been caused by several factors other than the influence of increased effective weight. For example, altered branchial muscle function and/or surface tension from droplets of residual water in the branchial chamber could impart forces not experienced in water (Vogel, 1984), or stiffening could result simply from dehydration of connective tissues (Avery and Bailey, 2008). By holding terrestrially acclimated fish under simulated microgravity, we explicitly tested the influence of body weight on gill mechanical properties. Simulated microgravity eliminated the stiffening response observed during normal terrestrial acclimation, strongly suggesting that gill arch stiffening during terrestrial acclimation is caused by increased effective body weight and not some other aspect of air exposure. Random positioning machines have been used successfully to mimic microgravity conditions in experiments using cultured cells (e.g. Kraft et al., 2000; Pardo et al., 2005; Patel et al., 2007), plants (Kittang et al., 2013) and invertebrates (Ricci and Boschetti, 2003), but to our knowledge this is the first successful ground-based simulation of microgravity for an adult vertebrate. Amphibious fishes such as

Journal of Experimental Biology (2017) 220, 3621-3631 doi:10.1242/jeb.161638

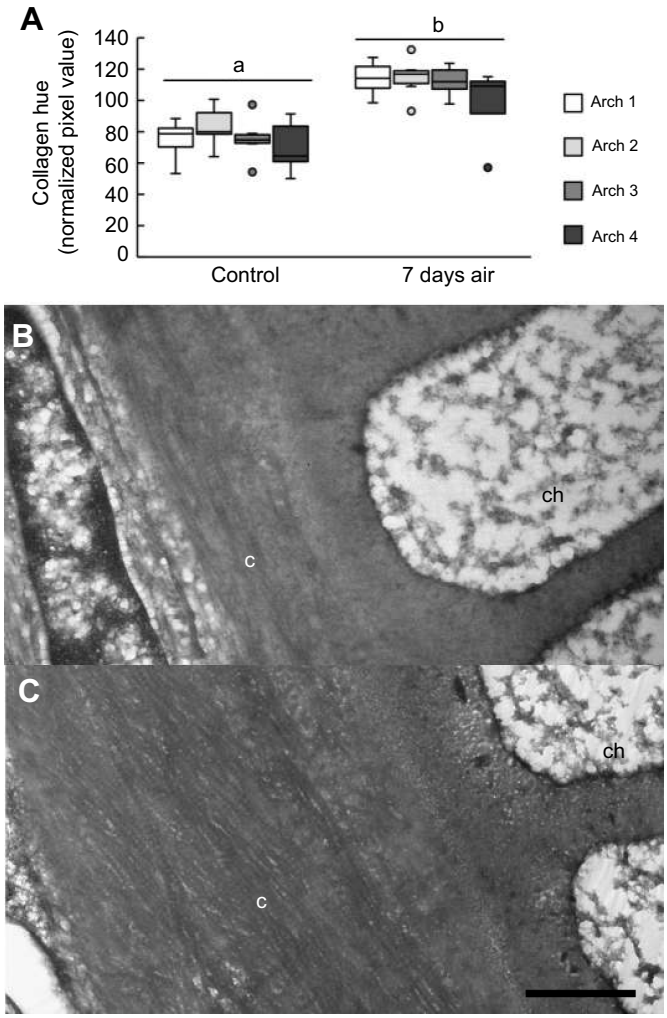

Fig. 6. Increased collagen density in mangrove rivulus gill filaments after terrestrial acclimation. (A) Boxplot showing the hue value of collagen measured in gill filament cross-sections; larger values indicate larger and more densely packed collagen fibrils (n=6 control and n=6 terrestrially acclimated fish; two-way repeated-measures ANOVA and Holm–Sidak *post hoc* tests P<0.001). (B,C) Representative transmission electron micrograph of a filament-supporting cartilaginous rod from a control fish in water (B) and from a fish acclimated terrestrially for 14 days (C). Note the diffuse and disorganized collagen (c) alongside the chondrocyte (ch) in the water-acclimated fish, which becomes more densely packed and organized after terrestrial acclimation. Scale bar, 1 µm.

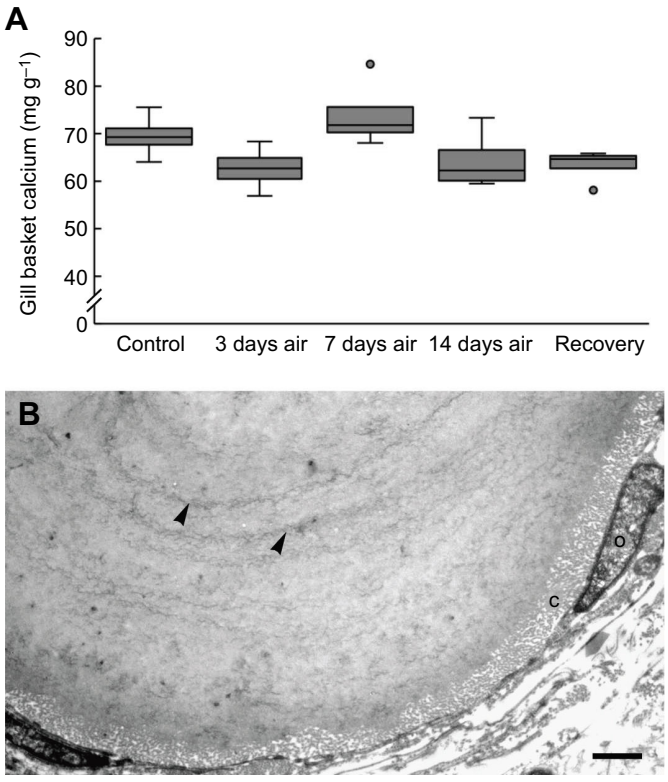

Fig. 7. Calcium content of *K. marmoratus* gill arches. (A) Boxplot showing the mean calcium content of gill baskets (n=4 samples for each time point; 5 gill baskets pooled per sample) from *K. marmoratus* acclimated to water (control) or over a time course of air exposure and recovery (one-way ANOVA P=0.045, but for all Holm–Sidak *post hoc* tests, P>adjusted critical P). (B) Transmission electron micrograph of a ceratobranchial bone cross-section of a control fish held in water, showing only a few dark mineralized bands (arrowheads). Diffuse collagen molecules (c) and osteoblasts (o) can be observed at the margin of the bone. Scale bar, 1 µm.

K. marmoratus may be a useful experimental model for future experiments investigating weight-induced musculoskeletal remodelling (Rea et al., 2016; Reilly and Franklin, 2016).

Adjustments to the morphology or mechanical properties of bones have widely been thought to require larger forces or strain rates than those imposed by gravitational loading (e.g. Frost, 1990; Aiello et al., 2015). However, sheep bones experimentally loaded with just 0.3 ***g*** of force have been shown to increase bone density and the rate of bone formation, demonstrating that even very small loads can be important for determining the mechanical properties of tissues (Rubin et al., 2001). Other studies in mammals have also shown that very low degrees of tissue strain are sufficient to cause skeletal remodelling (Sugiyama et al., 2012; Christen et al., 2014). Our results provide further evidence that very small mechanical signals, in this case increased effective weight in the absence of buoyant support from water, can modify skeletal morphology.

The prevalent mammalian view is that osteocytes, cells embedded within the bone matrix, are responsible for mechanosensitive responses in bone (Robling et al., 2006; Bonewald, 2011; Prideaux et al., 2016). In contrast, the bones of many teleosts including *K. marmoratus* lack osteocytes (Parenti, 1986; Shahar and Dean, 2013; Doherty et al., 2015). Without these mechanosensitive osteocytes, how can the ceratobranchial bones respond to increased effective body weight? In accordance with our results, several recent studies in other teleost fishes have demonstrated that anosteocytic bone can respond to changes in mechanical loading, suggesting that skeletal mechanosensitivity is more complicated than has been assumed (Witten and Huysseune, 2009; Shahar and Dean, 2013; Witten and Hall, 2015).

How are gill arches stiffened?

We used a combination of quantitative proteomics and histology to understand the morphological and biochemical changes underlying gill arch stiffening in terrestrially acclimated fish. Overall, our results indicate that stiffening of the gill arch skeleton in response to terrestrial acclimation is probably caused by complementary changes to the extracellular matrix of the gill arch skeleton, including growth via the synthesis and mineralization of new collagen plus the modification of existing matrix by the formation of cross-links. The changes to the extracellular matrix that occurred in *K. marmoratus* are also well known to occur in mammals in

Journal of Experimental Biology (2017) 220, 3621-3631 doi:10.1242/jeb.161638

response to changes in gravitational loading, such as during spaceflight (Humphrey et al., 2014).

Collagen is the main organic component of extracellular matrix and a major determinant of stiffness in bone and cartilage (Porter et al., 2006). Of the 1095 proteins identified in our proteomics analysis, type X collagen showed the largest increase in abundance of any protein. In mammals, type X collagen is a well-known marker for endochondral bone formation and ossification (Ricard-Blum et al., 2000; Shen, 2005). This protein is expressed by hypertrophic chondrocytes at the margins of growing endochondral bones, where it provides structural support and promotes mineralization (Jacenko et al., 1993; Rosati et al., 1994). Furthermore, experiments using cultured chondrocytes show that expression of type X collagen increases in response to mechanical strain (Yang et al., 2006). In fishes, type X collagen is similarly associated with bone formation (Renn and Winkler, 2010; Eames et al., 2012). Interestingly, in euteleost fishes, type X collagen is restricted to osteoblasts (Renn and Winkler, 2010), while in more basal fishes, including *D. rerio* and *Lepisosteus oculatus*, both chondrocytes and osteoblasts produce type X collagen (Eames et al., 2012). This suggests that common patterns of mechanically induced bone growth are found in all vertebrates, but there may be differences in the specific mesenchymal cells (chondrocytes versus osteoblasts) that are responsible for bone matrix deposition and mineralization in teleosts and mammals.

In addition to mineral density, cross-linking between collagen molecules in the extracellular matrix is an important determinant of the mechanical properties of bone (Oxlund et al., 1995; Banse et al., 2002; Avery and Bailey, 2008; Saito and Marumo 2010). Terrestrial acclimation of *K. marmoratus* increased the abundance of two collagen isoforms, types IX and XII, that enhance cross-linking and probably contributed to the observed increase in tissue stiffness. Type IX collagen coats the surface of other collagen fibrils and acts to bind the fibrillary network, which enhances structural integrity (Hulmes, 2008; Wess, 2008). Type XII is another cross-link forming collagen that is similarly localized to the surfaces of fibrils (Wess, 2008). This collagen isoform is upregulated by mechanical stress, regulates bone formation and is an important determinant of skeletal stiffness (Izu et al., 2011; Chiquet et al., 2014). Femurs of mutant mice lacking type XII collagen are less stiff than normal mice, and Picrosirius Red imaging of these bones indicated less organized and smaller collagen fibrils (Izu et al., 2011). Similarly, our histological evidence suggests that collagen was more densely packed and organized in terrestrially acclimated *K. marmoratus*, possibly facilitated by increased cross-linking owing to upregulation of types IX and XII collagen. Forming cross-links to stabilize existing extracellular matrix would provide a rapid and energetically inexpensive way to increase tissue stiffness that may complement the synthesis of new matrix (Oxlund et al., 1995).

There was no change in overall gill calcium content in response to terrestrial acclimation, suggesting large-scale mineralization is not responsible for gill arch stiffening. However, we noticed in several electron micrographs that a dark band of mineral was deposited at the margin of the ceratobranchial bones after terrestrial acclimation. This amount of additional mineral would probably be too small to be detectable in samples of whole gill arches, but may nevertheless be an important mechanism to increase stiffness. We were also surprised to find very low calcium content in the gill skeleton of mangrove rivulus (~17% dry mass), approximately half of what has been reported in other teleost fishes (Cohen et al., 2012). The low mineral content of *K. marmoratus* gills, however, is consistent with the relatively low forces required to deform the gill arches (Currey, 2003; Barak et al., 2013). Given the small and irregular nature of *K. marmoratus* gill arches, it was not possible to accurately determine Young's modulus – the material stiffness of a gill arch excluding effects of shape and size. However, using our Picrosirius-Red-stained sections we measured a mean gill arch cross-sectional area of 0.025±0.002 mm^2, which allowed us to calculate an approximate Young's modulus of 2–5 MPa. This value is closer to measurements of calcified cartilage in chondrichthyan vertebral centra (Porter et al., 2006) than to bones in other teleost fishes (Cohen et al., 2012). One possibility is that the skeletons of these tiny animals are adequately strong and stiff even with minimal mineralization owing to the relatively large cross-sectional area of the bones, which determines strength, compared with body size (Schmidt-Nielsen, 1984). The average mass of fish used in these experiments was 82±1 mg, at least 100 times smaller than other fishes in which bone mechanical properties and mineral density has been studied (Porter et al., 2006; Cohen et al., 2012).

Mechanosensitive responses to terrestrial acclimation may not be restricted to the gill arches of *K. marmoratus*, as we also saw evidence for structural remodelling at the level of the gill filaments and even within individual cells. Gill filaments are supported by cartilage rods (Wilson and Laurent, 2002), and terrestrial acclimation caused increased collagen density and organization within this cartilage in a manner that mirrored our results in the gill arches. Morphological adjustments at the level of the gill lamellae may also enhance structural support. In previous experiments, we have found that terrestrially acclimated *K. marmoratus* enlarge a mass of cells that fills the space between gill lamellae (Ong et al., 2007; LeBlanc et al., 2010; Turko et al., 2012). While the function of these cells has not been directly tested, one hypothesis is that this cell mass provides structural support out of water (Nilsson et al., 2012; Wright, 2012). Gill lamellae may also be supported by stiffening of the cytoskeleton. Our proteomics analysis showed increased abundance of actin and other proteins that regulate the microfilament network, which is thought to be the major determinant of intra-cellular mechanical properties (Rotsch and Radmacher, 2000) and may increase the stiffness of individual gill cells during terrestrial acclimation. Gill lamellar support may also be enhanced by laminins, which increased in abundance almost threefold in our study and provide structure to basement membranes of epithelia (Aumailley and Smyth, 1998).

Evolution of weight sensing in vertebrates

Considering the evolutionary history of effective weightlessness of fishes in water, it is intuitively reasonable to hypothesize that these animals are unable to sense body weight (Anken and Rahmann, 1999; Rahmann and Anken, 2002) and have skeletal systems unresponsive to changes in effective gravity (Martin, 2007). The different supportive requirements for animals in water versus on land have certainly influenced overall skeletal size – bone mass is related isometrically to body size in buoyant aquatic animals, while in terrestrial animals the relationship is exponential because bone strength is a function of cross-sectional area rather than volume (Reynolds, 1977; Schmidt-Nielsen, 1984). Furthermore, weight- and use-responsive musculoskeletal systems are not ubiquitous in tetrapods. In mice and humans, for example, skeletal mechanosensitivity is heritable and controlled by several genetic loci (Tajima et al., 2000; Kesavan et al., 2007; Kapur et al., 2010; Judex et al., 2013). Similarly, the musculoskeletal systems of many aestivating amphibians and hibernating mammals do not atrophy during months of inactivity (Doherty et al., 2015; Reilly and Franklin, 2016), suggesting the mechanosensitivity of support

structures may be shaped by selection. However, contrary to the hypothesis that weight-sensing originated with the tetrapod invasion of land, we found that the branchial skeleton of *K. marmoratus* stiffened in response to increased effective gravity during terrestrial acclimation using biochemical pathways similar to those known in mammals. We also recently reported reversible hypertrophy of aerobic body muscle in terrestrially acclimated *K. marmoratus* despite minimal activity, suggesting that weight-bearing responses are widespread throughout the musculoskeletal system (Brunt et al., 2016). Together, these data indicate that gravitational loading enhances body support in a teleost fish, despite an evolutionary history of effective weightlessness in water.

In the absence of time travel, it is impossible to know whether weight responsiveness in fishes represents the ancestral state. The ability of *K. marmoratus* to stiffen the gill skeleton when out of water may have evolved convergently with weight sensitivity in tetrapod bones to maintain structural integrity or prevent damage from weight bearing. More likely, considering the similarity of the proteomic response in the teleost *K. marmoratus* to the mechanisms used by tetrapods to remodel bone, the gravitational response we observed may indicate that the ability of bone-producing osteoblasts to respond to even slight changes in mechanical load is a fundamental feature of vertebrate skeletons (Shahar and Dean, 2013; Schilder, 2016). Mechanical stresses owing to differences in tissue density would occur even in neutrally buoyant, effectively weightless fishes, possibly providing an adaptive benefit to the ability to fine tune the skeleton. In amphibious fishes, similar fine-tuning of the skeleton would result in stiffer bones to provide body support, and if environmental conditions favoured highly terrestrial individuals, these plastic traits could become genetically assimilated in subsequent generations (Pigliucci et al., 2006; Standen et al., 2014). In support of this idea, we found that the gill arches of water-acclimated mangrove rivulus were stiffer than those of comparably sized zebrafish, a fully aquatic species, indicating that phenotypic plasticity may complement constitutively stiffer gill arches in the amphibious mangrove rivulus. It has also been hypothesized that novel mechanical forces acting on skeletons, such as gravity on the bones of fish out of water, could give rise to evolutionary innovations in bone structure (Danos and Staab, 2010). Mechanosensitive fish osteoblasts may have thus served as a valuable exaptation for producing a strong, stiff, weight-responsive skeleton during the tetrapod invasion of land (Khayyeri and Prendergast, 2013; Doherty et al., 2015).

Acknowledgements
We thank Andreas Heyland, Todd Gillis and Graham Scott, as well as Helen Coates (Ontario Veterinary College), Bob Harris (University of Guelph Electron Microscopy Unit), Peter Smith (University of Guelph School of Environmental Sciences Analytical Laboratory), Mike Davies and Matt Cornish (University of Guelph Hagen Aqualab).

Competing interests
The authors declare no competing or financial interests.

Author contributions
Conceptualization: A.J.T., D.F., P.A.W.; Methodology: A.J.T., D.K., D.F., R.P.C., F.M.S., M.R.S.; Validation: A.J.T., D.K.; Formal analysis: A.J.T., D.K.; Investigation: A.J.T., D.K., M.R.S.; Resources: D.K., R.P.C., F.M.S., P.A.W.; Data curation: D.K.; Writing - original draft: A.J.T.; Writing - review & editing: A.J.T., D.K., D.F., R.P.C., F.M.S., M.R.S., P.A.W.; Visualization: A.J.T.; Supervision: D.F., R.P.C., F.M.S., P.A.W.; Project administration: P.A.W.; Funding acquisition: A.J.T., D.K., R.P.C., P.A.W.

Funding
Funding was provided by a Canadian Society of Zoologists travel grant to A.J.T., Natural Sciences and Engineering Research Council of Canada (NSERC) Graduate Scholarships to A.J.T. and M.R.S., NSERC Discovery Grants to R.P.C. and P.A.W., and a National Science Foundation grant IOS-1355098 to D.K.

Data availability
Proteomics data are available at the MassIVE (accession no. MSV000080634) and ProteomeXchange (accession no. PXD006100) databases. Additional material, including the PEAKS Quant information, Scaffold file and other metadata are available at https://kueltzlab.ucdavis.edu/CAMP_dda_profiles.cfm?AC=CAMPDDA00013.

Supplementary information
Supplementary information available online at
http://jeb.biologists.org/lookup/doi/10.1242/jeb.161638.supplemental

References
Aiello, B. R., Iriarte-Diaz, J., Blob, R. W., Butcher, M. T., Carrano, M. T., Espinoza, N. R., Main, R. P. and Ross, C. F. (2015). Bone strain magnitude is correlated with bone strain rate in tetrapods: implications for models of mechanotransduction. *Proc. R. Soc. B Biol. Sci.* **282**, 20150321.
Anken, R. H. and Rahmann, H. (1999). Effect of altered gravity on the neurobiology of fish. *Naturwissenschaften* **86**, 155-167.
Atkins, A., Dean, M. N., Habegger, M. L., Motta, P. J., Ofer, L., Repp, F., Shipov, A., Weiner, S., Currey, J. D. and Shahar, R. (2014). Remodeling in bone without osteocytes: billfish challenge bone structure–function paradigms. *Proc. Natl Acad. Sci. USA* **111**, 16047-16052.
Atkins, A., Milgram, J., Weiner, S. and Shahar, R. (2015). The response of anosteocytic bone to controlled loading. *J. Exp. Biol.* **218**, 3559-3569.
Aumailley, M. and Smyth, N. (1998). The role of laminins in basement membrane function. *J. Anat.* **193**, 1-21.
Avery, N. C. and Bailey, A. J. (2008). Restraining cross-links responsible for the mechanical properties of collagen fibers: natural and artificial. In *Collagen Structure and Mechanics* (ed. P. Fratzl), pp. 81-110. New York: Springer.
Banse, X., Sims, T. J. and Bailey, A. J. (2002). Mechanical properties of adult vertebral cancellous bone: correlation with collagen intermolecular cross-links. *J. Bone Miner. Res.* **17**, 1621-1628.
Barak, M. M., Lieberman, D. E. and Hublin, J.-J. (2013). Of mice, rats and men: trabecular bone architecture in mammals scales to body mass with negative allometry. *J. Struct. Biol.* **183**, 123-131.
Berrar, D. P., Granzow, M. and Dubitzky, W. (2007). Introduction to genomic and proteomic data analysis. In *Fundamentals of Data Mining in Genomics and Proteomics* (ed. W. Dubitzky, M. Granzow and D. P. Berrar), pp. 1-38. New York: Springer.
Bonewald, L. F. (2011). The amazing osteocyte. *J. Bone Miner. Res.* **26**, 229-238.
Borst, A. G. and van Loon, J. J. W. A. (2009). Technology and developments for the random positioning machine, RPM. *Microgravity Sci. Technol.* **21**, 287-292.
Brunt, E. M., Turko, A. J., Scott, G. R. and Wright, P. A. (2016). Amphibious fish jump better on land after acclimation to a terrestrial environment. *J. Exp. Biol.* **219**, 3204-3207.
Chiquet, M., Birk, D. E., Bönnemannc, C. G. and Koch, M. (2014). Collagen XII: protecting bone and muscle integrity by organizing collagen fibrils. *Int. J. Biochem. Cell Biol.* **53**, 51-54.
Christen, P., Ito, K., Ellouz, R., Boutroy, S., Sornay-Rendu, E., Chapurlat, R. D. and van Rietbergen, B. (2014). Bone remodelling in humans is load-driven but not lazy. *Nat. Commun.* **5**, 4855.
Clack, J. A. (2002). *Gaining ground: The Origin and Evolution of Tetrapods*. Bloomington, IN: Indiana University Press.
Cohen, L., Dean, M., Shipov, A., Atkins, A., Monsonego-Ornan, E. and Shahar, R. (2012). Comparison of structural, architectural and mechanical aspects of cellular and acellular bone in two teleost fish. *J. Exp. Biol.* **215**, 1983-1993.
Cox, J. and Mann, M. (2008). MaxQuant enables high peptide identification rates, individualized ppb-range mass accuracies and proteome-wide protein quantification. *Nature Biotechnol.* **26**, 1367-1372.
Currey, J. D. (2002). *Gaining ground: The Origin and Evolution of Tetrapods*. Princeton, NJ: Princeton University Press.
Currey, J. D. (2003). The many adaptations of bone. *J. Biomech.* **36**, 1487-1495.
Danos, N. and Staab, K. L. (2010). Can mechanical forces be responsible for novel bone development and evolution in fishes? *J. Appl. Ichthyol.* **26**, 156-161.
Denny, M. W. (1993). *Air and Water: The Biology and Physics of Life's Media*. Princeton, NJ: Princeton University Press.
DiGirolamo, D. J., Kiel, D. P. and Esser, K. A. (2013). Bone and skeletal muscle: neighbors with close ties. *J. Bone Miner. Res.* **28**, 1509-1518.
Doherty, A. H., Ghalambor, C. K. and Donahue, S. W. (2015). Evolutionary physiology of bone: bone metabolism in changing environments. *Physiology* **30**, 17-29.
Eames, B. F., Amores, A., Yan, Y.-L. and Postlethwait, J. H. (2012). Evolution of the osteoblast: skeletogenesis in gar and zebrafish. *BMC Evol. Biol.* **12**, 27.
Frick, N. T. and Wright, P. A. (2002). Nitrogen metabolism and excretion in the mangrove killifish *Rivulus marmoratus* I. The influence of environmental salinity and external ammonia. *J. Exp. Biol.* **205**, 79-89.

Frost, H. M. (1990). Skeletal structural adaptations to mechanical usage (SATMU): 1. Redefining Wolff's law: the bone modeling problem. *Anat. Rec.* **226**, 403-413.
Fudge, D. S., Gardner, K. H., Forsyth, V. T., Riekel, C. and Gosline, J. M. (2003). The mechanical properties of hydrated intermediate filaments: insights from hagfish slime threads. *Biophys. J.* **85**, 2015-2027.
Herranz, R., Anken, R., Boonstra, J., Braun, M., Christianen, P. C. M., de Geest, M. Hauslage, J., Hilbig, R., Hill, R. J. A., Lebert, M. et al. (2013). Ground-based facilities for simulation of microgravity: organism-specific recommendations for their use, and recommended terminology. *Astrobiology* **13**, 1-17.
Hirt, C. and Featherstone, W. E. (2012). A 1.5 km-resolution gravity field model of the Moon. *Earth Planet. Sci. Lett.* **329-330**, 22-30.
Horn, E. R. (2005). Gravity effects on life processes in aquatic animals. *Adv. Space Biol. Med.* **10**, 247-301.
Hulmes, D. J. S. (2008). Collagen diversity, synthesis and assembly. In *Collagen Structure and Mechanics* (ed. P. Fratzl), pp. 15-48. New York: Springer.
Humphrey, J. D., Dufresne, E. R. and Schwartz, M. A. (2014). Mechanotransduction and extracellular matrix homeostasis. *Nat. Rev. Mol. Cell Biol.* **15**, 802-812.
Huysseune, A., Sire, J.-Y. and Meunier, F. J. (1994). Comparative study of lower pharyngeal jaw structure in two phenotypes of *Astatoreochromis alluaudi* (Teleostei: Cichlidae). *J. Morphol.* **221**, 25-43.
Izu, Y., Sun, M., Zwolanek, D., Veit, G., Williams, V., Cha, B., Jepsen, K. J., Koch, M. and Birk, D. E. (2011). Type XII collagen regulates osteoblast polarity and communication during bone formation. *J. Cell Biol.* **193**, 1115-1130.
Jacenko, O., LuValle, P. A. and Olsen, B. R. (1993). Spondylometaphyseal dysplasia in mice carrying a dominant negative mutation in a matrix protein specific for cartilage-to-bone transition. *Nature* **365**, 56-61.
Johnson, A. C., Turko, A. J., Klaiman, J. M., Johnston, E. F. and Gillis, T. E. (2014). Cold acclimation alters the connective tissue content of the zebrafish (*Danio rerio*) heart. *J. Exp. Biol.* **217**, 1868-1875.
Judex, S., Weidong, Z., Donahue, L. R. and Ozcivici, E. (2013). Genetic loci that control the loss and regain of trabecular bone during unloading and reambulation. *J. Bone Miner. Res.* **28**, 1537-1549.
Kapur, S., Amoui, M., Kesavan, C., Wang, X., Mohan, S., Baylink, D. J. and Lau, K.-H. W. (2010). Leptin receptor *(Lepr*) is a negative modulator of bone mechanosensitivity and genetic variations in *Lepr* may contribute to the differential osteogenic response to mechanical stimulation in the C57BL/6J and C3H/HeJ pair of mouse strains. *J. Biol. Chem.* **285**, 37607-37618.
Kelley, J. L., Yee, M.-C., Brown, A. P., Richardson, R. R., Tatarenkov, A., Lee, C. C., Harkins, T. T., Bustamante, C. D. and Earley, R. L. (2016). The genome of the self-fertilizing mangrove rivulus fish, *Kryptolebias marmoratus*: a model for studying phenotypic plasticity and adaptations to extreme environments. *Genome Biol. Evol.* **8**, 2145-2154.
Kesavan, C., Baylink, D. J., Kapoor, S. and Mohan, S. (2007). Novel loci regulating bone anabolic response to loading: expression QTL analysis in C57BL/6JXC3H/HeJ mice cross. *Bone* **41**, 223-230.
Khayyeri, H. and Prendergast, P. J. (2013). The emergence of mechanoregulated endochondral ossification in evolution. *J. Biomech.* **46**, 731-737.
King, J. A. C., Abel, D. C. and DiBona, D. R. (1989). Effects of salinity on chloride cells in the euryhaline cyprinodontid fish *Rivulus marmoratus*. *Cell Tissue Res.* **257**, 367-377.
Kittang, A.-I., Winge, P., van Loon, J. J. W. A., Bones, A. M. and Iversen, T.-H. (2013). Adaptation response of *Arabidopsis thaliana* to random positioning. *Adv. Space Res.* **52**, 1320-1331.
Kraft, T. F. B., van Loon, J. J. W. A. and Kiss, J. Z. (2000). Plastid position in *Arabidopsis* columella cells is similar in microgravity and on a random-positioning machine. *Planta* **211**, 415-422.
Kranenbarg, S., van Cleynenbreugel, T., Schipper, H. and van Leeuwen, J. (2005). Adaptive bone formation in acellular vertebrae of sea bass (*Dicentrarchus labrax* L.). *J. Exp. Biol.* **208**, 3493-3502.
Kültz, D., Li, J., Gardell, A. and Sacchi, R. (2013). Quantitative molecular phenotyping of gill remodeling in a cichlid fish responding to salinity stress. *Mol. Cell. Proteomics* **12**, 3962-3975.
Kültz, D., Li, J., Sacchi, R., Morin, D., Buckpitt, A. and Van Winkle, L. (2015). Alterations in the proteome of the respiratory tract in response to single and multiple exposures to naphthalene. *Proteomics* **15**, 2655-2668.
LeBlanc, D. M., Wood, C. M., Fudge, D. S. and Wright, P. A. (2010). A fish out of water: gill and skin remodeling promotes osmo-and ionoregulation in the mangrove killifish *Kryptolebias marmoratus*. *Physiol. Biochem. Zool.* **83**, 932-949.
Lyndon, A. R. and Houlihan, D. F. (1998). Gill protein turnover: costs of adaptation. *Comp. Biochem. Physiol.* **119**, 27-34.
MacKenna, D. A., Omens, J. H., McCulloch, A. D. and Covell, J. W. (1994). Contribution of collagen matrix to passive left ventricular mechanics in isolated rat hearts. *Am. J. Physiol. Heart Circ. Physiol.* **266**, 1007-1018.
Martin, R. B. (2007). The importance of mechanical loading in bone biology and medicine. *J. Musculoskelet. Neuronal Interact.* **7**, 48-53.
McBride, S. H. and Silva, M. J. (2012). Adaptive and injury response of bone to mechanical loading. *Bonekey Rep.* **1**, 192.
Meyer, A. (1987). Phenotypic plasticity and heterochrony in *Cichlasoma managuense* (Pisces, Cichlidae) and their implications for speciation in cichlid fishes. *Evolution* **41**, 1357-1369.
Nilsson, G. E., Dymowska, A. and Stecyk, J. A. W. (2012). New insights into the plasticity of gill structure. *Respir. Physiol. Neurobiol.* **184**, 214-222.
Ong, K. J., Stevens, E. D. and Wright, P. A. (2007). Gill morphology of the mangrove killifish (*Kryptolebias marmoratus*) is plastic and changes in response to terrestrial air exposure. *J. Exp. Biol.* **210**, 1109-1115.
Ord, T. J. and Cooke, G. M. (2016). Repeated evolution of amphibious behavior in fish and its implications for the colonization of novel environments. *Evolution* **70**, 1747-1759.
Oxlund, H., Barckman, M., Ortoft, G. and Andreassen, T. T. (1995). Reduced concentrations of collagen cross-links are associated with reduced strength of bone. *Bone* **17**, 365-371.
Pardo, S. J., Patel, M. J., Sykes, M. C., Platt, M. O., Boyd, N. L., Sorescu, G. P., Xu, M., van Loon, J. J. W. A., Wang, M. D. and Jo, H. (2005). Simulated microgravity using the Random Positioning Machine inhibits differentiation and alters gene expression profiles of 2T3 preosteoblasts. *Am. J. Physiol. Cell Physiol.* **288**, C1211-C1221.
Parenti, L. R. (1986). The phylogenetic significance of bone types in euteleost fishes. *Zool. J. Linn. Soc.* **87**, 37-51.
Patel, M. J., Liu, W., Sykes, M. C., Ward, N. E., Risin, S. A., Risin, D. and Jo, H. (2007). Identification of mechanosensitive genes in osteoblasts by comparative microarray studies using the rotating wall vessel and the random positioning machine. *J. Cell. Biochem.* **101**, 587-599.
Pigliucci, M., Murren, C. J. and Schlichting, C. D. (2006). Phenotypic plasticity and evolution by genetic assimilation. *J. Exp. Biol.* **209**, 2362-2367.
Porter, M. E., Beltrán, J. L., Koob, T. J. and Summers, A. P. (2006). Material properties and biochemical composition of mineralized vertebral cartilage in seven elasmobranch species (Chondrichthyes). *J. Exp. Biol.* **209**, 2920-2928.
Prideaux, M., Findlay, D. M. and Atkins, G. J. (2016). Osteocytes: the master cells in bone remodelling. *Curr. Opin. Pharmacol.* **28**, 24-30.
Rahmann, H. and Anken, R. H. (2002). Gravity related research with fishes-perspectives in regard to the upcoming international space station, ISS. *Adv. Space Res.* **30**, 697-710.
Rea, G., Cristofaro, F., Pani, G., Pascucci, B., Ghuge, S. A., Corsetto, P. A., Imbriani, M., Visai, L. and Rizzo, A. M. (2016). Microgravity-driven remodeling of the proteome reveals insights into molecular mechanisms and signal networks involved in response to the space flight environment. *J. Proteomics* **137**, 3-18.
Reilly, B. D. and Franklin, C. E. (2016). Prevention of muscle wasting and osteoporosis: the value of examining novel animal models. *J. Exp. Biol.* **219**, 2582-2595.
Renn, J. and Winkler, C. (2010). Characterization of *collagen type 10a1* and *osteocalcin* in early and mature osteoblasts during skeleton formation in medaka. *J. Appl. Ichthyol.* **26**, 196-201.
Reynolds, W. W. (1977). Skeleton weight allometry in aquatic and terrestrial vertebrates. *Hydrobiologia* **56**, 35-37.
Ricard-Blum, S., Dublet, B. and van der Rest, M. (2000). *Unconventional Collagens*. Oxford: Oxford University Press.
Ricci, C. and Boschetti, C. (2003). Bdelloid rotifers as model system to study developmental biology in space. *Adv. Space Biol. Med.* **9**, 25-39.
Rich, L. and Whittaker, P. (2005). Collagen and picrosirius red staining: a polarized light assessment of fibrillar hue and spatial distribution. *J. Morphol. Sci.* **22**, 97-104.
Robling, A. G., Burr, D. B. and Turner, C. H. (2001). Recovery periods restore mechanosensitivity to dynamically loaded bone. *J. Exp. Biol.* **204**, 3389-3399.
Robling, A. G., Castillo, A. B. and Turner, C. H. (2006). Biomechanical and molecular regulation of bone remodeling. *Annu. Rev. Biomed. Eng.* **8**, 455-498.
Rosati, R., Horan, G. S. B., Pinero, G. J., Garofalo, S., Keene, D. R., Horton, W. A., Vuorio, E., de Crombrugghe, B. and Behringer, R. R. (1994). Normal long bone growth and development in type X collagen-null mice. *Nature Genet.* **8**, 129-135.
Rotsch, C. and Radmacher, M. (2000). Drug-induced changes of cytoskeletal structure and mechanics in fibroblasts: an atomic force microscopy study. *Biophys. J.* **78**, 520-535.
Rubin, C., Turner, A. S., Bain, S., Mallinckrodt, C. and McLeod, K. (2001). Low mechanical signals strengthen long bones. *Nature* **412**, 603-604.
Saito, M. and Marumo, K. (2010). Collagen cross-links as a determinant of bone quality: a possible explanation for bone fragility in aging, osteoporosis, and diabetes mellitus. *Osteoporos. Int.* **21**, 195-214.
Schilder, R. J. (2016). (How) do animals know how much they weigh? *J. Exp. Biol.* **219**, 1275-1282.
Schmidt-Nielsen, K. (1984). *Scaling: Why is Animal Size so Important*. Cambridge: Cambridge University Press.
Schneider, C. A., Rasband, W. S. and Eliceiri, K. W. (2012). NIH Image to ImageJ: 25 years of image analysis. *Nat. Methods* **9**, 671-675.
Shahar, R. and Dean, M. N. (2013). The enigmas of bone without osteocytes. *BoneKEy Rep.* **2**, 343.
Shen, G. (2005). The role of type X collagen in facilitating and regulating endochondral ossification of articular cartilage. *Orthod. Craniofacial. Res.* **8**, 11-17.

Journal of Experimental Biology

Standen, E. M., Du, T. Y. and Larsson, H. C. E. (2014). Developmental plasticity and the origin of tetrapods. *Nature* **513**, 54-58.

Sugiyama, T., Meakin, L. B., Browne, W. J., Galea, G. L., Price, J. S. and Lanyon, L. E. (2012). Bones' adaptive response to mechanical loading is essentially linear between the low strains associated with disuse and the high strains associated with the lamellar/woven bone transition. *J. Bone Miner. Res.* **27**, 1784-1793.

Tajima, O., Ashizawa, N., Ishii, T., Amagai, H., Mashimo, T., Liu, L. J., Saitoh, S., Tokuyama, K. and Suzuki, M. (2000). Interaction of the effects between vitamin D receptor polymorphism and exercise training on bone metabolism. *J. Appl. Physiol.* **88**, 1271-1276.

Tatarenkov, A., Ring, B. C., Elder, J. F., Bechler, D. L. and Avise, J. C. (2010). Genetic composition of laboratory stocks of the self-fertilizing fish *Kryptolebias marmoratus*: a valuable resource for experimental research. *PLoS ONE* **5**, e12863.

Taylor, D. S. (2012). Twenty-four years in the mud: what have we learned about the natural history and ecology of the mangrove rivulus, *Kryptolebias marmoratus*? *Integr. Comp. Biol.* **52**, 724-736.

Turko, A. J., Cooper, C. A. and Wright, P. A. (2012). Gill remodelling during terrestrial acclimation reduces aquatic respiratory function of the amphibious fish *Kryptolebias marmoratus*. *J. Exp. Biol.* **215**, 3973-3980.

Turko, A. J., Robertson, C. E., Bianchini, K., Freeman, M. and Wright, P. A. (2014). The amphibious fish *Kryptolebias marmoratus* uses different strategies to maintain oxygen delivery during aquatic hypoxia and air exposure. *J. Exp. Biol.* **217**, 3988-3995.

Turner, C. H. (1998). Three rules for bone adaptation to mechanical stimuli. *Bone* **23**, 399-407.

Ueki, M., Tanaka, N., Tanimoto, K., Nishio, C., Honda, K., Lin, Y.-Y., Tanne, Y., Ohkuma, S., Kamiya, T., Tanaka, E. et al. (2008). The effect of mechanical loading on the metabolism of growth plate chondrocytes. *Ann. Biomed. Eng.* **36**, 793-800.

Vogel, S. (1984). *Life in Moving Fluids: The Biology of Flow*. Princeton, NJ: Princeton University Press.

Wess, T. J. (2008). Collagen fibrillar structure and hierarchies. In *Collagen Structure and Mechanics* (ed. P. Fratzl), pp. 49-80. New York: Springer.

Wilson, J. M. and Laurent, P. (2002). Fish gill morphology: inside out. *J. Exp. Zool.* **293**, 192-213.

Witten, P. E. and Hall, B. K. (2015). Teleost skeletal plasticity: modulation, adaptation, and remodelling. *Copeia* **103**, 727-739.

Witten, P. E. and Huysseune, A. (2009). A comparative view on mechanisms and functions of skeletal remodelling in teleost fish, with special emphasis on osteoclasts and their function. *Biol. Rev.* **84**, 315-346.

Wright, P. A. (2012). Environmental physiology of the mangrove rivulus, *Kryptolebias marmoratus*, a cutaneously breathing fish that survives for weeks out of water. *Integr. Comp. Biol.* **52**, 792-800.

Wright, P. A. and Turko, A. J. (2016). Amphibious fishes: evolution and phenotypic plasticity. *J. Exp. Biol.* **219**, 2245-2259.

Wuest, S. L., Richard, S., Kopp, S., Grimm, D. and Egli, M. (2015). Simulated microgravity: critical review on the use of random positioning machines for mammalian cell culture. *Biomed. Res. Int.* **2015**, 971474.

Yang, X., Vezeridis, P. S., Nicholas, B., Crisco, J. J., Moore, D. C. and Chen, Q. (2006). Differential expression of type X collagen in a mechanically active 3-D chondrocyte culture system: a quantitative study. *J. Orthop. Surg.* **1**, 15.

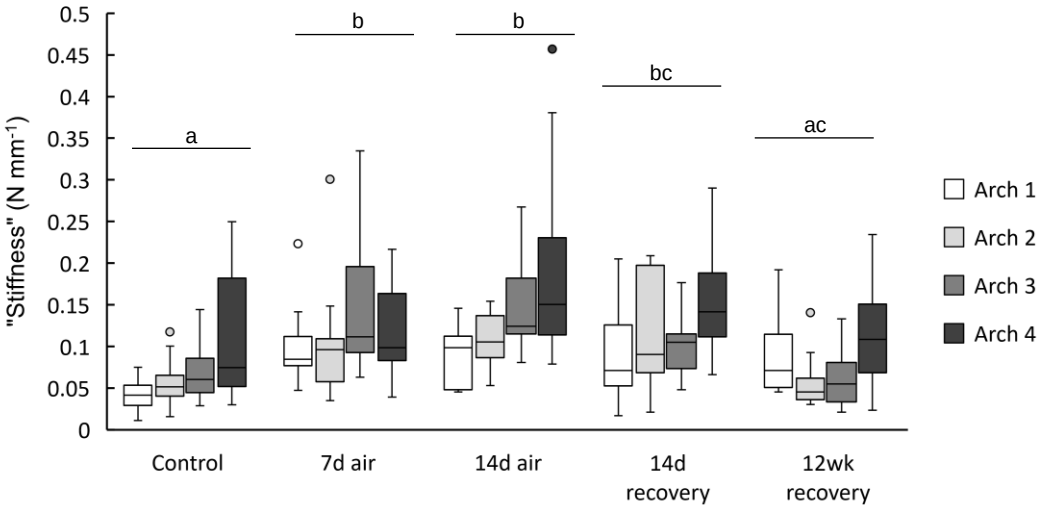

Fig. S1. Increased gill stiffness (calculated as a spring constant from force/length curves) after terrestrial acclimation is reversible in *K. marmoratus*. Force relative to gill arch length required to deform all four gill arches from the left side of control fish in water (n=15), after 7d (n=13) or 14d in air (n=13), or 14d in air followed by 14d (n=12) or 12 weeks (n=12) recovery in water. Different letters above treatment groups denote significant effects of treatment (two-way repeated-measures ANOVA and Holm-Sidak *post hoc* tests, P<0.001).

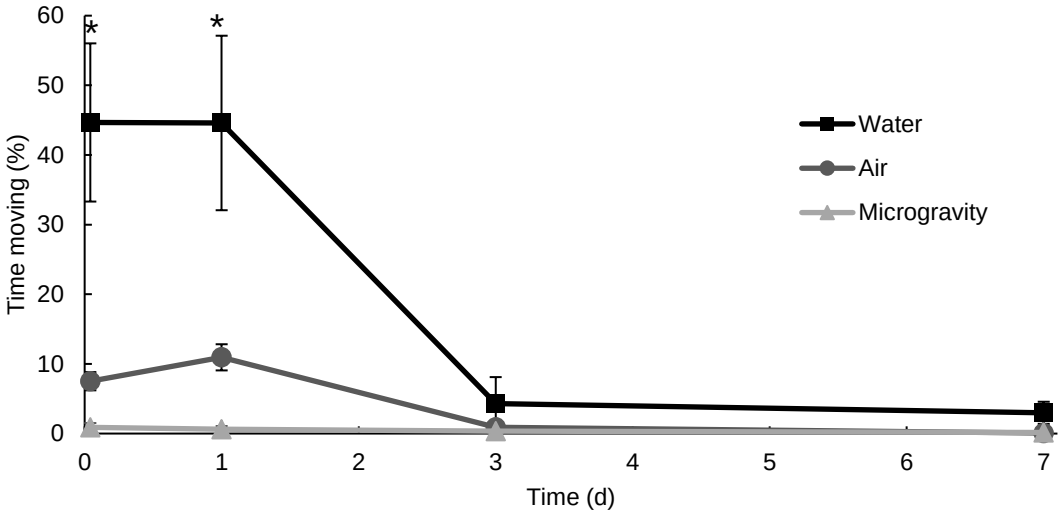

Fig. S2. Activity of mangrove rivulus in the simulated microgravity experiment. Control fish in water (black line; *n*=6) reduced activity to levels comparable to terrestrially-acclimated fish after 3 d of acclimation to a 6-well plate. Terrestrially-acclimated fish moved infrequently under both normal gravity conditions (dark grey line; *n*=6), and when exposed to simulated microgravity in the random positioning machine (light grey line; *n*=6). All fish were fasted for the duration of the experiment. Asterisks denote significant differences between water-acclimated and each terrestrially-acclimated group within a time point (repeated measures ANOVA and Holm-Sidak *post hoc* tests, treatment*time

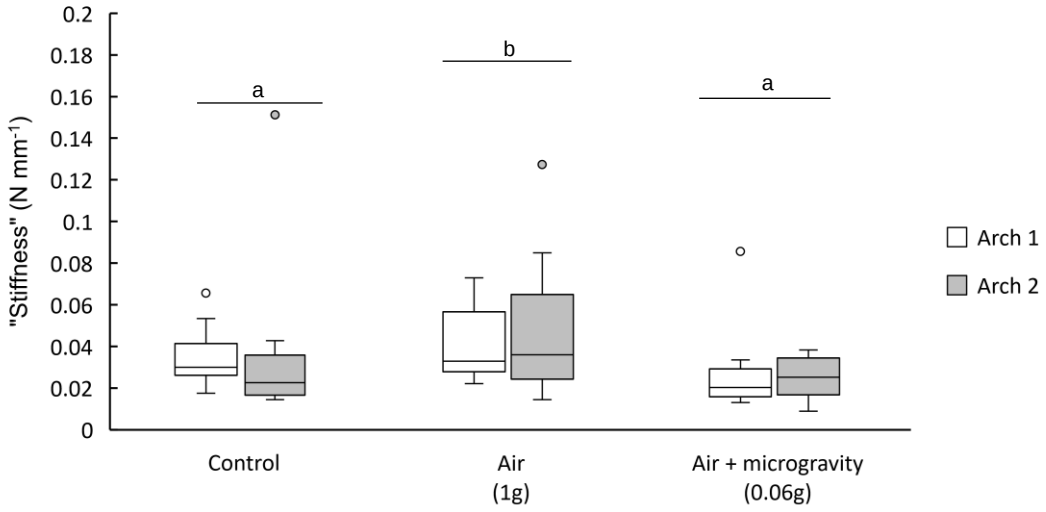

Fig. S3. Increased gill stiffness (calculated as a spring constant from force/length curves) after terrestrial acclimation in *K. marmoratus* does not occur in simulated microgravity. Force relative to gill arch length required to deform gill arches 1 and 2 in fish acclimated to water at 1*g* (*n*=12), 7d in air at 1*g* (*n*=12), or 7d in simulated microgravity (0.06*g*; *n*=10). Different letters above treatment groups denote significant effects of treatment (two-way repeated-measures ANOVA and Holm-Sidak *post hoc* tests, *P*=0.025).

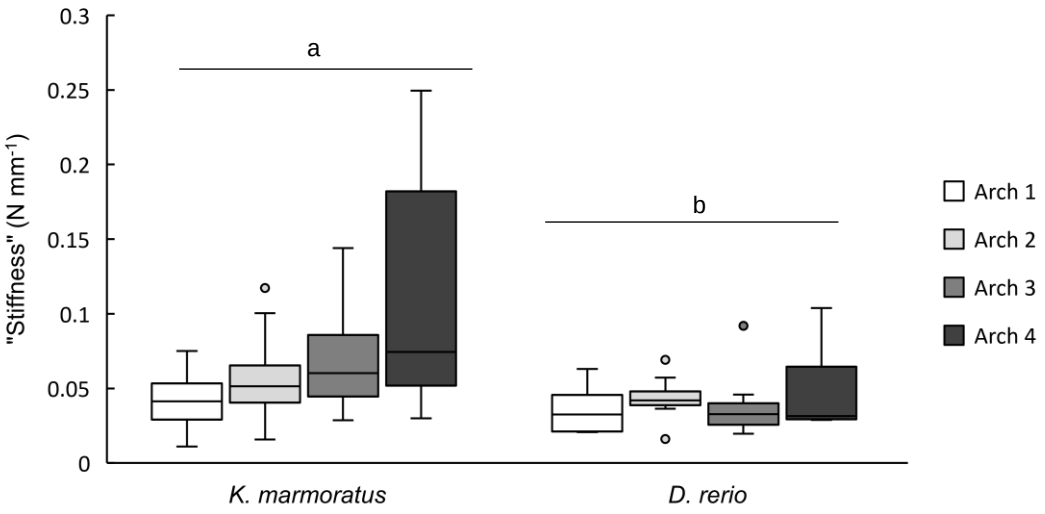

Fig. S4. Increased gill stiffness (calculated as a spring constant from force/length curves) of *K. marmoratus* versus *D. rerio* gill arches. Force relative to gill arch length required to deform gill arches from the left side of amphibious *K. marmoratus* acclimated to water (n=15) compared to those of the fully aquatic zebrafish (n=9). The *K. marmoratus* data presented here are the control values repeated from Fig. S1 for comparison. Different letters above treatment groups denote significant differences between species (two-way repeated-measures ANOVA and Holm-Sidak *post hoc* tests, P=0.006).

Table S1. Abundances of all collagen isoforms identified in the gills of *Kryptolebias marmoratus* acclimated to water or 14d in air.

NCBI Accession	Protein annotation	Coverage (%)	#Peptides	#Unique	Relative abundance (air/water)	P value
gi|1041063337	collagen alpha-2(I) chain	67	80	75	1.03	0.2041737945
gi|1041090756	collagen alpha-1(I) chain-like isoform X1	55	73	67	1.3	0.0000426580
gi|1041065690	collagen alpha-1(I) chain-like	50	70	66	1.33	0.0000012589
gi|1041073117	collagen alpha-1(II) chain isoform X2	12	13	10	1.09	0.0398107171
gi|1041074737	collagen alpha-1(II) chain-like isoform X2	4	5	2	0.89	0.0002398833
gi|1041075806	collagen alpha-2(IV) chain isoform X2	2	3	2	0.88	0.0028183829
gi|1041145053	collagen alpha-4(IV) chain-like	1	1	1	1.26	0.0000013804
gi|1041075808	collagen alpha-1(IV) chain	3	4	3	1.65	0.0001819701
gi|1041138366	collagen alpha-6(IV) chain-like	2	4	3	1.23	0.0034673685
gi|1041132849	collagen alpha-2(V) chain	8	12	9	0.99	0.7762471166
gi|1041125201	collagen alpha-1(V) chain-like isoform X2	5	9	6	1.2	0.0000012882
gi|1041106386	collagen alpha-1(VI) chain	33	33	32	1.24	0.0000676083
gi|1041145385	collagen alpha-3(VI) chain partial	27	56	55	1.2	0.0001096478
gi|1041106315	collagen alpha-2(VI) chain-like	33	37	33	1.18	0.4897788194
gi|1041145452	collagen alpha-3(VI) chain-like partial	23	39	37	1.1	0.0257039578
gi|1041113033	collagen alpha-2(VI) chain-like isoform X2	20	19	18	1.01	0.4677351413
gi|1041138699	collagen alpha-3(VI) chain-like partial	17	25	25	1.05	0.1348962883
gi|1041145951	collagen alpha-4(VI) chain-like partial	23	15	15	1.19	0.1621810097
gi|1041141506	collagen alpha-2(V) chain-like	12	12	11	1.13	0.0000933254
gi|1041063832	collagen alpha-2(IX) chain	5	3	1	0.61	0.0263026799
gi|1041119925	collagen alpha-1(IX) chain-like isoform X3	2	1	1	2.37	0.0000000000
gi|1041126807	collagen alpha-1(IX) chain-like	2	1	1	0.77	0.3801893963
gi|1041074889	collagen alpha-3(IX) chain isoform X1	2	2	1	0.89	0.0000000000
gi|1041062211	collagen alpha-1(X) chain-like	2	1	1	8.84	0.0000000000
gi|1041144154	collagen alpha-1(X) chain-like	3	1	1	1.69	0.0000000000
gi|1041118682	collagen alpha-1(XI) chain-like isoform X2	6	9	5	0.95	0.2398832919
gi|1041088438	collagen alpha-1(XI) chain-like	8	13	8	1.26	0.0011748976
gi|1041059509	collagen alpha-1(XI) chain-like	3	5	1	1.02	0.0000000000
gi|1041061459	collagen alpha-1(XII) chain isoform X2	25	72	65	0.74	0.0004365158
gi|1041140211	collagen alpha-1(XII) chain-like partial	17	19	18	0.98	0.1778279410
gi|1041146700	collagen alpha-1(XII) chain-like isoform X1	8	2	1	2.35	0.0000000000
gi|1041147096	collagen alpha-1(XII) chain-like	4	1	1	0.88	0.0056234133
gi|1041146058	collagen alpha-1(XII) chain-like partial	6	6	3	1.16	0.0025703958
gi|1041148375	collagen alpha-1(XII) chain-like partial	6	2	2	1.26	0.8511380382

Movie 1. Time lapse video of *K. marmoratus* during acclimation to microgravity in the random positioning machine. Images were captured every 2s and are played back at 60x speed.